5474 J. Med. Chem. 2009, 52, 5474–5484
DOI: 10.1021/jm9007104

Journal of Medicinal Chemistry Article

Studies of the Mechanism of Action of Platinum(II) Complexes with Potent Cytotoxicity in Human Cancer Cells

Anwen M. Krause-Heuer,[†] Renate Grünert,[‡] Sybill Kühne,[‡] Magdalena Buczkowska,[‡] Nial J. Wheate,[†] Delphine D. Le Pevelen,[§] Leanne R. Boag,[†] Dianne M. Fisher,[∥] Jana Kasparkova,[⊥] Jaroslav Malina,[⊥] Patrick J. Bednarski,[‡] Viktor Brabec,[⊥,#] and Janice R. Aldrich-Wright*,[†]

[†]*Nanoscale Organisation and Dynamics Group, School of Biomedical and Health Sciences, University of Western Sydney, Locked Bag 1797, Penrith South DC, 1797, NSW, Australia,* [‡]*Institute of Pharmacy, University of Greifswald, 17487 Greifswald, Germany,* [§]*Chiralabs Ltd., Oxford University, Begbroke Science Park, Oxfordshire OX5 1PF, U.K.,* [∥]*School of Chemistry, University of Sydney, NSW, 2006, Australia,* [⊥]*Institute of Biophysics, Academy of Sciences of the Czech Republic, v.v.i., Kralovopolska 135, CZ-61265 Brno, Czech Republic, and* [#]*Laboratory of Biophysics, Department of Experimental Physics, Faculty of Sciences, Palacky University, CZ-77146 Olomouc, Czech Republic*

Received May 25, 2009

We have examined the biological activity of 12 platinum(II)-based DNA intercalators of the type $[Pt(I_L)(A_L)]^{2+}$, where I_L is an intercalating ligand (1,10-phenanthroline or a methylated derivative) and A_L is an ancillary ligand (diaminocyclohexane, diphenylethylenediamine or 1,2-bis(4-fluorophenyl)-1,2-ethylenediamine). The chiral compounds (**1**−**9**) and the racemic compounds (**10**−**12**) were tested against a panel of human cancer cell lines, with a number of complexes displaying activity significantly greater than that of cisplatin (up to 100-fold increase in activity in the A-427 cell line). The activity of the complexes containing diphenylethylenediamine (**8** and **9**) and 1,2-bis(4-fluorophenyl)-1,2-ethylenediamine (**10**−**12**) was significantly lower compared to the complexes containing diaminocyclohexane (**1**−**7**). Further in vitro testing, such as DNA unwinding, competition assays, and DNase 1 footprinting, was conducted on the most active compound (**5**) and its enantiomer (**6**) to provide information about the mechanism of action. These complexes display activity in cisplatin resistant cell lines, have higher cellular uptake than cisplatin, and do not activate caspase-3 as cisplatin does, indicating that these complexes exhibit a different mechanism of action.

Introduction

Since the discovery of cisplatin, thousands of platinum compounds have been synthesized and evaluated for antitumor activity. For many years, the driving force in platinum drug design has been the investigation of previously described structure−activity relationships. More recently there have been successful efforts to prepare compounds that disobey the "classical" structure−activity relationships.[1,2] We have developed a group of platinum(II)-based DNA intercalators of the type $[Pt(I_L)(A_L)]^{2+}$ (where I_L[a] is an intercalating ligand and A_L is an ancillary ligand), some of which demonstrate significant potential against human cell lines in vitro, including those that show resistance to current chemotherapeutic agents.[3−8] With these compounds we have shown that the type and chirality of the ancillary ligand, along with functional group substitution on the intercalating ligand, play an important role in cytotoxic activity. An interesting structural feature of these new cytotoxic platinum complexes is the absence of anionic ligands (e.g., chloride) that serve as leaving groups in traditional platinum antitumor agents that act by platination of DNA. Instead, the coordination spheres of these platinum complexes are filled with four relatively stable, bound nitrogens of two chelating ligands.[9] Thus, it would not appear that covalent binding between the platinum complex and DNA is responsible for their potent cytotoxicity.

In previous studies we have reported the cytotoxicity of a number of these compounds **1**−**7** (as the perchlorate salts) in a variety of cell lines[7] as well as the cytotoxicity of the water-soluble compounds in the murine leukemia (L1210) cell line.[3,6,10] To date, our lead compound, [(5,6-dimethyl-1,10-phenanthroline)(1*S*,2*S*-diaminocyclohexane)platinum(II)]$^{2+}$ (**5**), displays cytotoxicity up to 100-fold greater than that of cisplatin in the L1210 cell line. On the basis of these studies, we believe that further investigations of the biological activity of **5** and related compounds is required in order to gain further insight into the mechanism of action and the way that these compounds overcome cisplatin resistance. We have also synthesized compounds with the ancillary ligand 1,2-diphenylethanediamine (**8** and **9**) and fluorinated derivatives (**10**,

*To whom correspondence should be addressed. Phone: +61 2 4620 3218. Fax: +61 2 4620 3025. E-mail: j.aldrich-wright@uws.edu.au.

[a] Abbreviations: 3,4,7,8-Me_4phen, 3,4,7,8-tetramethyl-1,10-phenanthroline; 5,6-Me_2phen, 5,6-dimethyl-1,10-phenanthroline; 5637, human bladder cancer cell line; 5-Mephen, 5-methyl-1,10-phenanthroline; A-427, human lung cancer cell line; AAS, atomic absorption spectroscopy; A_L, ancillary ligand; AMC, 7-amino-4-methylcoumarin; bfed, 1,2-bis(4-fluorophenyl)-1,2-ethanediamine; ct-DNA, calf thymus-DNA; DAN-G, pancreas cancer cell line; dped, 1,2-diphenylethanediamine; ESI-MS, electrospray ionization mass spectrometry; EtBr, ethidium bromide; HL-60, human leukemia cell line; I_L, intercalating ligand; L1210, murine leukemia cell line; LCLC-103H, large cell human lung cancer cell line; MCF-7, human breast cancer cell line (hormone dependent); MDB-MB 231, human breast cancer cell line (hormone independent); MTT, 3-(4,5-dimethylthiazol-2-yl)-2,5-diphenyltetrazoliumbromide; NMR, nuclear magnetic resonance spectroscopy; phen, 1,10-phenanthroline; *R,R*-dach, 1*R*,2*R*-diaminocyclohexane; RP-HPLC, reverse-phase high pressure liquid chromatography; RT-4, urinary bladder transitional cell carcinoma cell line; *S,S*-dach, 1*S*,2*S*-diaminocyclohexane.

 Published on Web 08/06/2009

11, **12**). These ligands have been used to mimic the synthetic estrogens diethylstilbestrol and hexestrol in an attempt to target the estrogen receptor system.[11−14] [1,2-Diarylethanediamine]platinum(II) compounds have displayed activity in a number of hormone dependent (MCF-7) and independent (MDB-MB 231) breast cancer cell lines.[15−17] The most active in vivo were the meso and racemic derivatives of [1,2-bis-2,6-difluoro-3-hydroxyphenyl)ethylenediamine]sulfatoplatinum(II),[15] although these compounds did not display significant activity in vitro.[18] As such, it was of interest to determine whether the addition of a phenanthroline intercalating ligand to the molecule would produce a more cytotoxic compound.

In this study we report the synthesis and characterization of five new complexes: [(5,6-dimethyl-1,10-phenanthroline)(1*S*,2*S*-diphenylethylenediamine)platinum(II)]$^{2+}$ (**8**); [(5,6-dimethyl-1,10-phenanthroline)(1*R*,2*R*-diphenylethylenediamine) platinum(II)]$^{2+}$ (**9**) and the racemic compound [(1,10-phenanthroline)(1,2-bis(4-fluorophenyl)-1,2-ethylenediamine)platinum(II)]$^{2+}$ (**10**); [(5-methyl-1,10-phenanthroline)(1,2-bis(4-fluorophenyl)-1,2-ethylenediamine)platinum-(II)]$^{2+}$ (**11**) and [(5,6-dimethyl-1,10-phenanthroline)(1,2-bis-(4-fluorophenyl)-1,2-ethanediamine)platinum(II)]$^{2+}$ (**12**). The in vitro activity of compounds (**1**−**12**) was assessed against six human cancer cell lines, 5637 (human bladder cancer), RT-4 (urinary bladder transitional cell carcinoma), A-427 (human lung cancer), LCLC-103H (large cell human lung cancer), DAN-G (pancreatic cancer), and MCF-7 (human breast cancer), to further investigate whether the same structure−activity relationship is observed compared to that already seen in the L1210 cell line.

The potential of **5** and **6** as anticancer drugs has been established by in vitro cytotoxicity studies; however, further testing is required to elucidate a possible mechanism of action. Although DNA may be the ultimate target for these metal complexes, DNA binding experiments have shown no noticeable stereoselectivity in their binding affinities.[3] It has been hypothesized that differing cellular uptake rates may determine how much of the intercalating complexes enters the cell, thereby affecting cytotoxicity.[6] We have investigated the platinum uptake rates in the 5637 bladder cancer cell line, where a 2-fold difference in cytotoxicity between the enantiomers (**5** and **6**) was observed. The pair was assessed for cross-resistance using two cisplatin resistant cells lines (SISO-CDDP from human cervical cancer and KYSE-70-CDDP from human esophageal cancer). Caspase-3 activation studies, DNA unwinding experiments, competition assays, and DNase I footprinting were also performed to further investigate the DNA modifications caused by **5** and **6**.

Results and Discussion

Synthesis. Complexes **1**−**7** (Figure 1) were synthesized using a previously published method, and in each case the NMR spectra were comparable to those previously reported.[10] The synthesis of **8** and **9** was initially attempted via the method used for **1**−**7**. This method, however, proved to be unsuccessful, as the complex could not be purified with a C-18 reverse phase column. The yellow band of the metal complex could not be eluted and remained at the head of the column. This was likely due to the increased aromaticity of the ligand. As such, the synthesis of **8**−**12** (Figure 1) was carried out by coordinating the intercalating ligand first.[3,19,20]

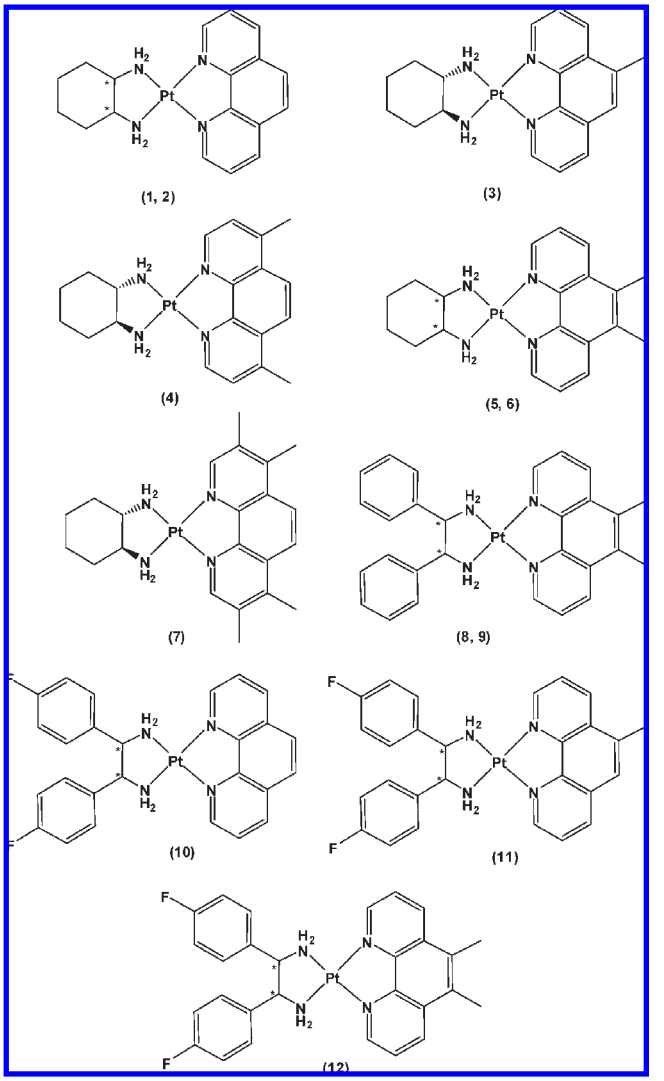

Figure 1. Chemical structures of the platinum(II)-based DNA intercalating complexes synthesized as part of this study. Stereocenters are indicated by an asterisk (∗) and are either *S* or *R*. Charges and counterions have been omitted for clarity; however, all charges are +2, with chloride or perchlorate counterions.

This involved reacting potassium tetrachloroplatinate (K_2PtCl_4) with 1 mol equiv of I_L in DMSO to produce [Pt(I_L)Cl_2], then refluxing this complex with 2 mol equiv of the ancillary ligand in water. The complex was precipitated with sodium perchlorate and washed with water, ethanol, and diethyl ether to remove the unreacted ancillary ligand. The conversion of complexes **8** and **9** to the water-soluble chloride salt was attempted using various anion exchange resins; however, isolation of the pure chloride form of the complexes was not achieved, and as such, the biological activity of these complexes was assessed as their perchlorate salt.

Complexes **10**−**12** were successfully converted to the water-soluble salts by stirring with anion exchange resin in water with gentle heating, followed by removal of the resin by filtration and removal of the water under reduced pressure.

X-ray Crystal Structure Determination of Metal Complex 10. The structure of complex **10** ({[Pt(phen)(*rac*-bfed)]Cl_2·[Pt(phen)(*rac*-bfed)]$NiCl_4$}·4H_2O, $(CH_3)_2CO$ shown in Figure 2) was determined by single crystal X-ray diffraction.

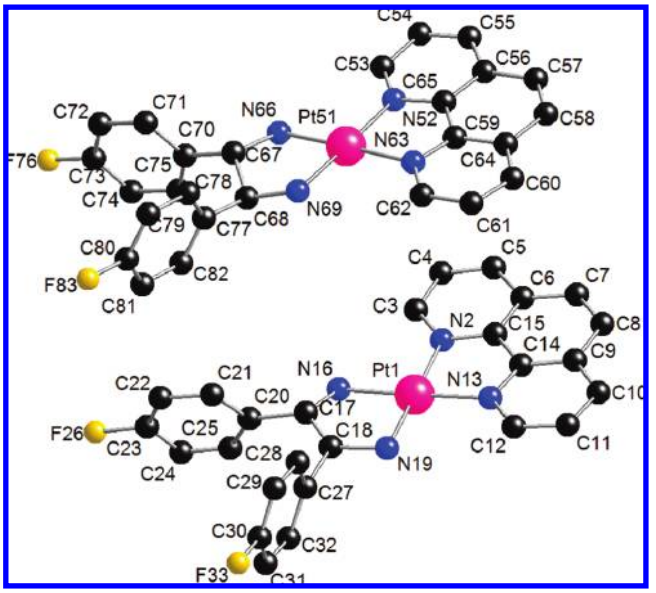

Figure 2. X-ray crystal structure of **10**, displaying the atom numbering scheme. Hydrogen atoms are omitted for clarity.

Table 1. Structural Parameters and Crystallographic Data for Metal Complex **10**

parameter	
molecular formula	$C_{55}H_{58}Cl_6F_4N_8NiO_5Pt_2$
molecular mass	1648.71
crystal system	triclinic
space group	$P\bar{1}$ (No. 2)
a (Å)	10.7001(1)
b (Å)	14.93992(1)
c (Å)	21.7791(3)
V (Å^3)	3049.66(6)
α (deg)	107.4540(5)
β (deg)	94.2428(5)
γ (deg)	105.0112(6)
D_c (g cm^{-3})	1.793
Z	2
crystal size (mm^3)	0.02 × 0.06 × 0.70
absorption coefficient (mm^{-1})	5.209
F(000)	1608.00
crystal color	yellow
crystal habit	blade
λ(Mo Kα) (Å)	0.71073
$T_{(Gaussian)min,max}$	0.73−0.90
θ range for data collection (deg)	5.1− 27.5
hkl range	$-13 \le h \le 13$, $-18 \le k \le 18$, $-28 \le l \le 28$
N	25205
N_{ind}	25205
N_{obs}	14159
N_{var}	730
completeness to θ	26.702 (99.2%)
final R indices [$I > 3\sigma(I)$]	R1(F)=0.0398, wR2(F)=0.0411
goodness-of-fit on S	1.1024

The crystallographic parameters are presented in Table 1, and further information is available in the Supporting Information. Complex **10** was triclinic, with each asymmetric unit containing two metal complex molecules, one $NiCl_4$ molecule, and two chloride counterions, with an acetone molecule and four water molecules associated with each enantiomeric pair. The H atoms were all located in a difference map except those attached to carbon atoms which were repositioned geometrically. The chloride and nickel chloride counterions, which are required to balance the +2 charge of each of the metal complexes, were associated with one or the other of the individual platinum complexes in the crystal structure. Complex **10** was found to have a distorted square-planar geometry around the central metal atom. The coordination geometry is essentially square planar, with distortion caused by the steric constraints imparted by the bidentate 1,10-phenanthroline ligand.

The N−Pt−N bond angles, Pt−N bond lengths, and N−C−C−N torsion angles observed in the complex molecules are summarized in Table 2. The N−Pt−N bond angles of the coordinated 1,10-phenanthroline in the independent molecules 1 and 51 (81.1(2)° and 81.2(2)°, respectively) are comparable with those previously reported for the crystal structure of [Pt(*S,S*-dach)(phen)]$(ClO_4)_2 \cdot 1.5H_2O$ (81.08(14)° and 81.28(15)°)[7] and other analogous complexes[7,19,21] with bond angles ranging between 80.3° and 81.7°. Likewise, the observed Pt−N (phen) bond lengths (between 2.014(5) and 2.033(5) Å, Table 2) are also consistent with those found in the analogous $[Pt(diamine)(phen)]^{2+}$ crystal structures, ranging between 2.01 and 2.05 Å.[7,19] The crystals were grown from a racemic mixture of metal complex (a mixture of *S,S* or *R,R* conformation of ancillary ligands). The metal complex molecules stack in alternate conformations, i.e., *S,S*-bfed followed by *R,R*-bfed (in a 2 + 2 stacking arrangement, as shown in red and blue in Figure S1, Supporting Information). Three water molecules (containing O45, O46, and O47) are hydrogen-bonded to the platinum complex (Pt1) through the two amino groups, and the four chlorine atoms of the $NiCl_4$ (namely, Cl35, Cl37, Cl39, and Cl40) are in proximity. The fourth water molecule (containing O200) is hydrogen-bonded to the other platinum complex (complex Pt51). The acetone molecule is also in close contact with the platinum complex Pt51 (Figure S2, Supporting Information). The metal complex molecules are $\pi-\pi$ stacked in a head-to-tail arrangement with an intermolecular spacing between the two molecules of ~3.4 Å.

Growth Inhibition Assays. To estimate the in vitro antitumor potential of the complexes, antiproliferative activity was determined in a panel of six human tumor cell lines: 5637 and RT-4 (human bladder cancer); A427 and LCLC-103H (human lung cancer); DAN-G (human pancreatic cancer); MCF-7 (human breast cancer); and A2780 (human ovarian cancer). A well established microtiter assay was used to measure the antiproliferative effects of the complexes.[22] The complexes were initially screened at 20 μM to determine whether further testing for IC_{50} values was warranted; complexes failing to inhibit cell growth by more than 50% at this concentration were considered inactive in the respective cell line.

The results of the cytotoxicity assays (Table 3) presented some interesting structure−activity relationships. The stereochemistry of the 1,2-diaminocyclohexane ring (dach) is critical for good activity, with the *S,S* enantiomers (**1** and **5**) being 5- to 10-fold more active than their *R,R* counterparts (**2** and **6**). The cytotoxicity of **1** is improved by the introduction of methyl substituents on the phenanthroline ligand. The number and position of methyl substituents on the phenanthroline ligand are important for cytotoxicity, with mono- and dimethylated phenanthroline complexes in the 5 or 5,6 positions (**3** and **5**) being the most active, followed by dimethylation in the 4,7 positions (**4**), which are all generally more active than the tetramethylated complex (**7**). The most active complexes (**3** and **5**) displayed IC_{50} values below

Table 2. N−Pt−N Bond Angles and Bond Lengths and N−C−C−N Torsion Angles for Metal Complex **10**

N−Pt−N Bond Angles			
atoms	angle (deg)	atoms	angle (deg)
N2−Pt1−N13	81.1(2)	N52−Pt51−N63	81.2(2)
N2−Pt1−N16	98.0(2)	N52−Pt51−N66	98.5(2)
N2−Pt1−N19	178.3(2)	N52−Pt51−N69	177.7(2)
N13−Pt1−N16	178.5(2)	N63−Pt51−N66	177.5(2)
N13−Pt1−N19	98.5(2)	N63−Pt51−N69	98.2(2)
N16−Pt1−N19	82.3(2)	N66−Pt51−N69	82.2(2)
Pt−N Bond Lengths			
atoms	distance (Å)	atoms	distance (Å)
Pt1−N2	2.015(5)	Pt51−N52	2.015(5)
Pt1−N13	2.014(5)	Pt51−N63	2.025(5)
Pt1−N16	2.032(5)	Pt51−N66	2.033(5)
Pt1−N19	2.026(5)	Pt51−N69	2.025(5)
N−C−C−N Torsion Angles			
atoms	angle (deg)	atoms	angle (deg)
N2−C15−C14-N13	1.1(9)	N52−C65−C64-N63	−4.4(8)
N16−C17−C18-N19	50.0(7)	N66−C67−C68-N69	36.1(11)

Table 3. IC_{50} Values in Seven Human Cancer Cell Lines (Averages of at Least Three Independent Experiments ± SD)[a]

		cell line, IC_{50} (nM)						
compd	chirality	5637	RT-4	A-427	LCLC-103H	DAN-G	MCF-7	HL-60
1	*SS*	91 ± 8	880 ± 640	110 ± 50	nd	nd	150 ± 80	nd
2	*RR*	540 ± 440	2950 ± 790	1190 ± 850	nd	nd	250 ± 140	nd
3	*SS*	**46 ± 2**	**106 ± 14**	**19 ± 5**	**47 ± 17**	57 ± 11	**35 ± 8**	nd
4	*SS*	**43 ± 4**	127 ± 15	48 ± 8	60 ± 20	**46 ± 4**	39 ± 4	nd
5	*SS*	82 ± 29*	**59 ± 10**	**21 ± 12**	**46 ± 13**	**40 ± 3**	**28 ± 4**	487 ± 162
6	*RR*	171 ± 89*	313 ± 46	214 ± 72	251 ± 15	238 ± 13	97 ± 3	6370 ± 1190
7	*SS*	143 ± 49	136 ± 24	26 ± 4	144 ± 40	169 ± 9	34 ± 12	nd
8	*SS*	2960 ± 3270	11590 ± 5400	2460 ± 1900	2570 ± 2390	5580 ± 2580	2670 ± 500	nd
9	*RR*	1220 ± 640	8470 ± 540	2520 ± 440	3340 ± 1030	8060 ± 2290	1560 ± 40	nd
10	*rac*	10860 ± 2910	> 20000	> 20000	15720 ± 4380	> 20000	> 20000	nd
11	*rac*	5450 ± 560	> 20000	> 20000	6960 ± 2060	> 20000	> 20000	nd
12	*rac*	2110 ± 480	11880 ± 1980	3070 ± 440	1750 ± 350	4630 ± 540	7970 ± 2920	nd
cisplatin**		350 ± 100	1610 ± 160	1969 ± 540	900 ± 190	730 ± 340	1380 ± 290	407 ± 90*
[Pt(*rac*-dach)Cl_2]**	*rac*	820 ± 190	170 ± 110	930 ± 270	570 ± 230	950 ± 740	230 ± 130	nd

[a] The two most active compounds in each cell line are emphasised in bold. nd: not determined. (*) $p < 0.002$ (paired, two-tailed t test, $N = 5$). (**) Values from ref 22.

100 nM in the majority of the cell lines tested and are 8- to 100-fold more active than cisplatin in these cell lines. Complex **5** was the most active compound in the majority of cell lines and was considerably more active than cisplatin and [Pt(*rac*-dach)Cl_2] (Table 3). The exception is in the HL60 cell line, where cisplatin was more active (Table 3).

Cisplatin analogues with 1,2-diphenylethylenediamine (dped) ligands have previously been shown to possess potent antitumor activity.[11,13,23] As shown in this work, the addition of 1,10-phenanthroline (and methylated derivatives) to [Pt(*rac*-dach)Cl_2] yielded a more active compound than the platinum complex [Pt(*rac*-dach)Cl_2] (Table 3). Thus, the compounds (**8** and **9**) containing the ancillary ligand 1,2-diphenylethanediamine[11,13] and the racemic para-fluorinated derivative[11−16] (bfed) (**10**, **11**, **12**) were synthesized to see if the substitution of the two chlorides for a phenanthroline intercalating ligand would produce platinum coordination complexes with more potent cytotoxic activity.

The complexes with dach (**5** and **6**) are consistently more potent than those with either enantiomer of dped (**8** and **9**). In these dped complexes, the stereochemistry of the ancillary ligand is not as important for activity but in general the *R,R* enantiomer is slightly more active. The *rac*-[1,2-bis(4-fluorophenyl)ethylenediamine]dichloroplatinum(II) complex [Pt(bfed)Cl_2] has been reported to have activity comparable to that of cisplatin.[9,11−16] In this work when 1,10-phenathroline was added to [Pt(bfed)Cl_2], the resulting complex **10** was less active than [Pt(bfed)Cl_2], with an IC_{50} over 20 μM in a number of cell lines. The activity of the fluorinated derivates can be partially restored by methylation of the phenanthroline ligand, with the 5,6 dimethylated complex (**12**) being the most active of the series. This reduction in activity upon the addition of the intercalator is the opposite trend to what has been observed for compounds **5**−**9**.

Cisplatin Resistant Cell Lines. The activity of the enantiomeric pair **5** and **6** was further investigated in two cisplatin resistance cell lines (SISO human cervical cancer and KYSE-70 human esophagus cancer). SISO-CDDP and KYSE-70-CDDP display 4- and 2.9-fold resistance to cisplatin, respectively, compared to the native line. In the case of SISO-CDDP, no cross-resistance was seen with the more active complex **5** while the less active enantiomer **6** showed a low level of cross-resistance (Table 4). On the other hand, neither isomer showed cross-resistance with the KYSE-70 cell line,

Table 4. IC_{50} Values (nM) for Complexes **5** and **6** in Two CDDP Resistant Cell Lines (Values Are Averages of at Least Three Independent Experiments ± SD)

	IC_{50} (nM)			
compd	SISO	SISO-CDDP (RF[a] = 4.0)	KYSE-70	KYSE-70-CDDP (RF[a] = 2.9)
5	23 ± 15	23 ± 8	20 ± 3	16 ± 4
6	83 ± 20	122 ± 21	161 ± 47	143 ± 24

[a] RF is the resistance factor for cisplatin in the respective cell lines.

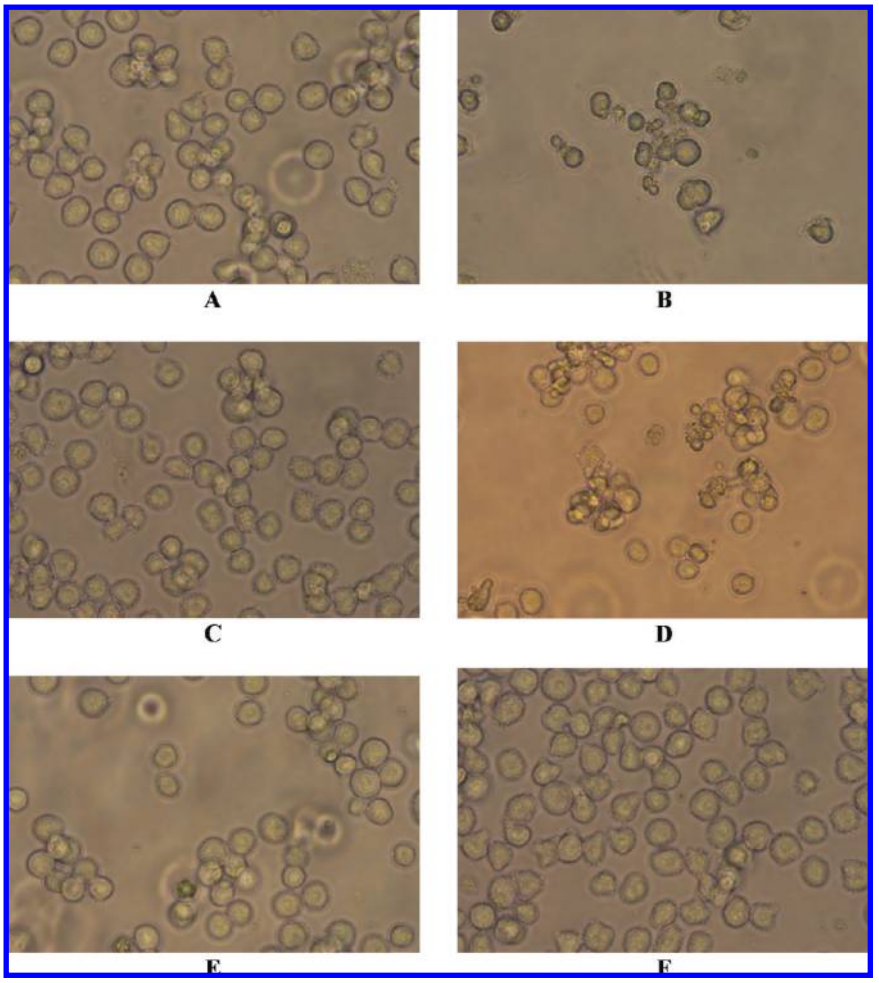

Figure 3. Photographs of HL-60 cells (400× magnification) showing the morphological changes when the cells are treated with **5** and **6** compared with etoposide. Cells were untreated (A) or treated 24 h with 2 μM etoposide (B), 0.5 μM **5** (C), 2.0 μM **5** (D), 0.5 μM **6** (E), or 2 μM **6** (F). The morphologies of HL-60 cells treated with 2.0 μM 56MESS show similar changes compared to cells treated with 2.0 μM etoposide, i.e., cell membrane shrinkage, blebbing, and apoptotic bodies.

and in fact, the cells resistant to cisplatin were slightly more sensitive to the complexes **5** and **6** than the native line. The results indicate that complexes **5** and **6** act by a mechanism of action different from that of cisplatin or that **5** and **6** are less susceptible to the mechanisms of cisplatin resistance. As such, further attempts were made to understand the possible differences in the mechanism(s) of action between **5**, **6**, and cisplatin.

Caspase-3 Activation Assay. Apoptosis is a frequently reported mechanism by which anticancer agents induce cell death. We have therefore investigated whether the effecter caspase-3 is activated when HL-60 human leukemia cells are exposed to **5** and **6**. As seen with the cancer cells originating from solid tumors, the HL-60 cells showed the same enantiomeric selective cytotoxicity for **5** over **6** (Table 3). Both cisplatin and etoposide are efficient activators of caspase-3 like activity in HL-60 cells at their IC_{90} values (data not shown). At the IC_{50} and IC_{90} values for **5** (0.5 and 3 μM), however, neither **5** nor **6** caused any measurable increase in the caspase-3 like activity of the HL-60 cells after 24 h (data not shown). Nevertheless, HL-60 cells exposed to 2 μM **5** for 24 h did show obvious morphological changes, similar to those seen with etoposide, such as membrane cell shrinkage, blebbing, and the formation of apoptotic bodies (Figure 3). Thus, caspase-3 activation does not appear to be an important event in cell death caused by **5**. For complex **6**, the concentration of 2 μM was still well below the IC_{50} value in the HL-60 line (Table 3) and explains why no cell death was observed.

Cellular Platinum Uptake. The platinum uptake of cisplatin, **5**, and **6** (25 μM) was tested in 5637 human bladder cancer cells. Over the first 4 h no differences were observed in the uptake rates of platinum for the two enantiomeric complexes **5** and **6** (Figure 4). At 6 h the uptake of **5** increased

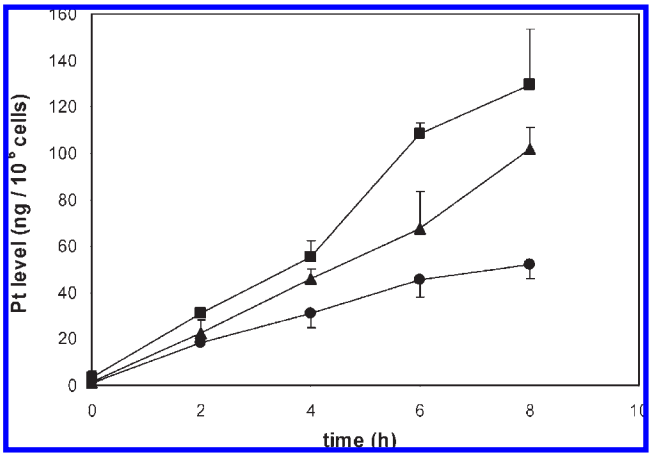

Figure 4. Uptake of cisplatin (●), **5** (■), and **6** (▲) in the 5637 cell line. Cells were treated with 25 μM Pt complexes at 37 °C for the times shown. Results are the averages of three independent experiments ± SD. Only half the error bars are displayed for clarity.

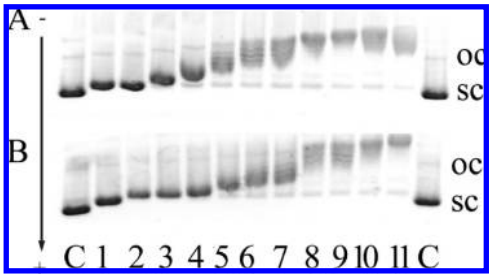

Figure 5. Unwinding of negatively supercoiled pSP73 plasmid DNA by **6** (A) and **5** (B): lane C, control (nonmodified DNA); (A, B) lanes 1−11, platinum complex/base ratio = 0.01, 0.02, 0.03, 0.04, 0.05, 0.06, 0.07, 0.08, 0.09, 0.1, 0.12, respectively. sc and oc (open circle) indicate supercoiled and relaxed (nicked) forms of plasmid DNA.

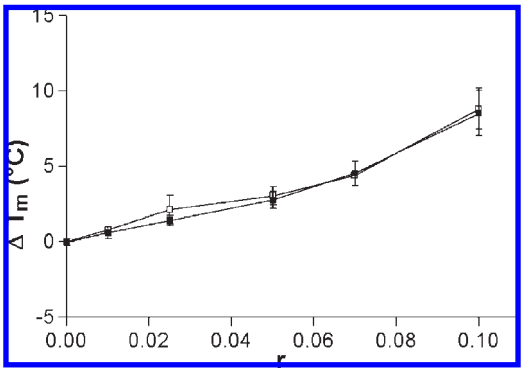

Figure 6. Plots showing the dependence of ΔT_m values on r for calf thymus DNA modified by **5** (□) and **6** (■). The melting curves were measured in a medium of 10 mM Tris-HCl at pH 7.4 and varying concentrations of complex. ΔT_m is defined as the difference between the T_m values of platinated and nonmodified DNAs. Data were measured in triplicate, and standard deviation is shown in the graph.

over **6**, but by 8 h the difference was negligible when the error in the measurements is taken into account. These data would seem to indicate that the 2-fold difference in antiproliferative activity of **5** over **6** in the 5637 cell line (Table 3) is not a result of varying rates of drug uptake by the cells. For cisplatin (at the same concentration) the uptake of total platinum is approximately half that of **5** and **6**. Although these dicationic

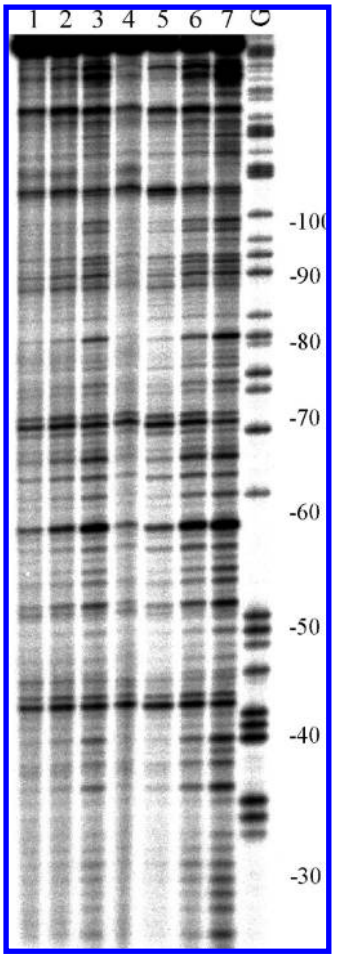

Figure 7. Autoradiogram of DNase I footprint of 3′ end labeled strand of 161 bp fragment from pBluescript SK(−) in the presence of different concentrations of **5** (lanes 1−3) and **6** (lanes 4−6). Lanes 1−3: DNA mixed with **5** at 8:1, 10:1, and 20:1 (base/complex) ratios, respectively. Lanes 4−6: DNA mixed with **6** at 8:1, 10:1, and 20:1 ratios, respectively. Lane 7: DNA in the absence of compound. Lane G corresponds to Maxam−Gilbert G ladder. Numbers refer to the sequence shown in the corresponding differential cleavage plots in Figure 8.

platinum intercalators presumably cannot cross the cell membrane by simple diffusion, they are taken up more readily than the neutral cisplatin. The significant difference in the cytotoxicity between **5** and cisplatin, however, cannot be due to differences in the amounts of drug taken up by the cells alone. These results support those obtained from the caspase-3 activity assay, which suggest that **5** and cisplatin have different mechanisms of actions.

Unwinding of Negatively Supercoiled DNA. Figure 5 shows the electrophoresis gels where a mixture of relaxed and negatively supercoiled pSP73 plasmid DNA (2464 bp) has been treated with increasing amounts of **5** and **6**. The unwinding angle is given by $\Phi = 18\sigma/r(c)$, where σ is the superhelical density and $r(c)$ is the number of platinum complexes bound per nucleotide at which the supercoiled and relaxed forms comigrate. The number of platinum complexes bound per nucleotide was taken to be equal to the mixing ratios based on the assumption that all molecules present in the sample are completely bound to the DNA.

This assumption is substantiated by high values of the apparent binding constants ($K_{app} > 1 \times 10^5\ M^{-1}$) determined for binding of the **5** or **6** enantiomer, respectively, to DNA

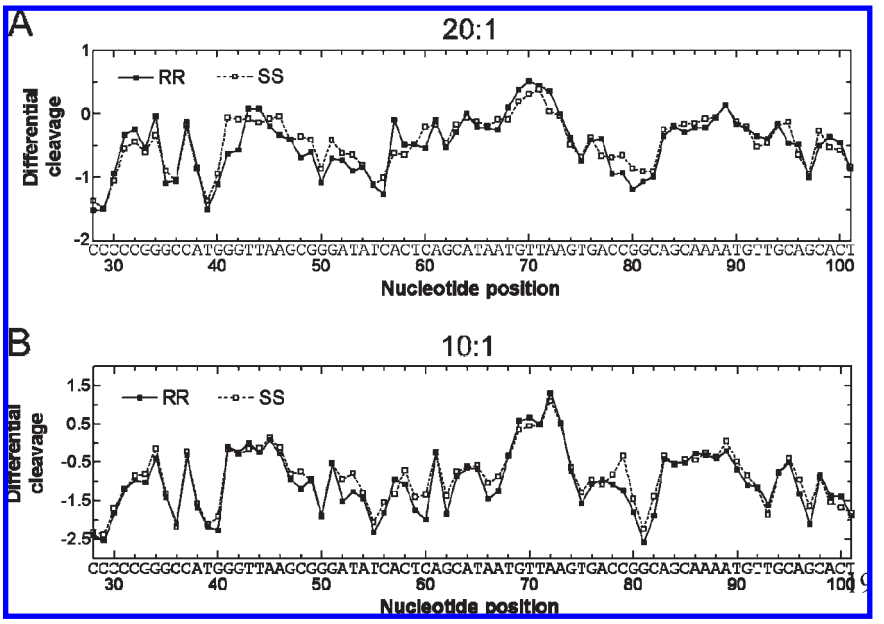

Figure 8. Differential cleavage plots for **5** (□) and **6** (■) induced differences in susceptibility to DNase I digestion of the 161 bp fragment at (A) 20:1 (DNA base/platinum complex) and (B) 10:1 ratios. Vertical scales are in units of $\ln(f_c) - \ln(f_0)$, where f_c is the fractional cleavage at any bond in the presence of compound and f_0 is the fractional cleavage of the same bond in the control, given closely similar extents of overall digestion. Positive values indicate enhancement, and negative values indicate inhibition.

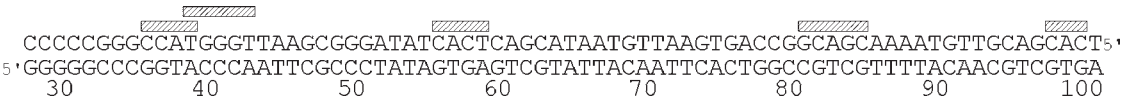

Figure 9. Part of the 161 bp fragment sequence showing preferential binding sites (shown as light bars) of **5** and **6** at DNA base/platinum complex ratio (20:1). The binding sites were obtained by extending the sites of inhibited DNase I cleavage by one nucleotide on both sides and shifting by 2 bp in the 3′ direction.

with a random nucleotide sequence. Under the present experimental conditions, σ was calculated to be −0.037, based on data for cisplatin where the r(c) was determined in this study and the literature value of $\Phi = 13°$ was assumed.[24] By use of this approach, DNA unwinding angles of 5.6 ± 0.7° and 7.4 ± 1.0° were determined for **5** and **6**, respectively. The unwinding angle is smaller than that of ethidium bromide (EtBr) at 26° or [2-hydroxyethanethiolato (2,2′,2″-terpyridine)platinum(II)] at ∼18.5° but is similar to the small arene compound [(η^6-*p*-cymene)Ru(ethylenediamine)(Cl)]$^+$ at 7 ± 0.5°.[24−26] The modest unwinding angle indicates that the platinum complexes, **5** or **6**, do not insert deeply into the base pair stack.

Thermal Stability of DNA. Melting of DNA modified by complex **5** or **6** (Figure 6) also deserves discussion. The following factors may account for the enhancement of thermal stability of DNA modified by **5** or **6**:[26] (1) the stabilizing effects of the positive charge on platinum and favorable stacking interactions between the base residues and the 5,6-dimethyl-1,10-phenanthroline group; (2) the separation of negative charges of the DNA backbone due to insertion of the 5,6-dimethyl-1,10-phenanthroline group (resulting in the elongation and unwinding of DNA). That is, changes in solvent structure and the counterion distribution around the phosphate groups may help to overcome electrostatic forces that do not favor the hybridization of the strands of the duplex.[27,28]

DNase I Footprinting. Complexes **5** and **6** were mixed with the 161 bp restriction fragment of pBluescript SK(−) phagemid at various ratios of base/complex (8:1, 10:1, and 20:1) followed by partial cleavage by DNase 1. The autoradiogram of the DNA cleavage inhibition patterns for **5** and **6** (Figure 7) shows that the extent of DNase I cleavage varies along the DNA sequence and that the cutting is strongly reduced in several places, even in the absence of the platinum complexes (Figure 7, lane 7). In the presence of the platinum complexes, **5** or **6**, no strong footprints in the gel can be seen. In order to obtain detailed information about the binding specificities of both enantiomers, intensities from gel lanes containing DNA and **5** or **6** at 20:1 and 10:1 ratios were measured by densitometry. The resulting differential cleavage plots are shown in Figure 8. Negative values indicate sites of drug protection from DNase I cleavage and positive values regions of drug-induced enhancement of cleavage. A stretch of DNA (∼70 bp) within the 161 bp restriction fragment was sufficiently well resolved to provide quantitative data. It can be seen that both enantiomers exhibit very similar patterns of protection and enhancement for both ratios 20:1 (Figure 8A) and 10:1 (Figure 8B). Since no additional lower affinity sites can be detected at higher concentrations of **5** and **6** and the size of footprints is also not increased, a ratio of 20:1 was chosen for analysis of the preferential binding sites. The strongest sites of DNase I cleavage inhibition correspond to the sequences 3′-GC (35−36), 3′-ATG (38−40), 3′-TC (55−56), 3′-GGC (80−82), and single nucleotide G (97). To identify the sites of drug binding from the sites of inhibited DNase I cleavage, a 3′-shift of about 2−3 bp must be considered because of the bias introduced by the nuclease upon DNA cleavage.[29] The resulting binding sites of both enantiomers at 20:1 were

extended by one nucleotide on both sides. Interestingly, closer inspection reveals that all binding sites contain 3′-CA dinucleotides at 37−38, 39−40, 56−57, 83−83, and 98−99 positions (Figure 9).

Conclusions

We have examined the biological activity of 12 platinum(II) metallointercalators of the type $[Pt(I_L)(A_L)]^{2+}$ (where I_L is an intercalating ligand and A_L is an ancillary ligand). The IC_{50} values in seven human cancer lines indicated that complexes **1**−**7**, which include the 1,2-diaminocyclohexane ligand, were more active than cisplatin and [Pt(*rac*-dach)Cl_2] in all but one (HL60) of the cell lines. The compounds incorporating the 1*S*,2*S*-diaminocyclohexane (**5**) ancillary ligand were more active than the comparable compounds containing 1*S*,2*S*-diphenylethanediamine (**8**) and *rac*-1,2-bis(4-fluorophenyl)-1,2-ethylenediamine (**12**) in the 5637 cell line. This was unexpected, since [Pt(bfed)Cl_2] displays activity in MCF and MDA-MB 231 breast cancer cell lines.[13−16] The stereochemistry of the ancillary ligand has an effect on the overall activity of the metal complex, with the *S*,*S* enantiomer often being more active than the *R*,*R* compound (e.g, **1** and **2**, **5** and **6**), although this trend is not observed with all ancillary ligands (e.g., **8** and **9**).

While many of the complexes were more active than cisplatin we examined the enantiomeric pair **5** and **6** in order to probe the mechanism of action. Neither **5** nor **6** caused any measurable increase in caspase-3 activity, unlike cisplatin or etoposide. As the route to cell death in the HL-60 cells does not involve caspase-3 activation, it appears likely that apoptosis is not the mechanism for cell death. Cellular platinum uptake experiments revealed that while **5** and **6** were taken up into the cell at approximately the same rate, both are taken up more readily than cisplatin. These experiments indicate that the mechanism of action of **5** is different from that of cisplatin. Experiments including unwinding of negatively supercoiled DNA showed only insignificant differences between **5** and **6**, which do not explain the significant differences in cytotoxicity. DNase I footprinting revealed only small differences between **5** and **6**, and interestingly all binding sites identified contain the 3′-CA dinucleotide. These experiments have not revealed why **5** is more cytotoxic than **6**, as such further investigation is needed to uncover the reasons for such marked differences in cytotoxicity.

Experimental Section

Materials. 1*S*,2*S*-Diaminocyclohexane, 1*R*,2*R*-diaminocyclohexane, 1*S*,2*S*-diphenylethylenediamine, 1*R*,2*R*-diphenylethylenediamine, 1,10-phenanthroline (phen), 5-methyl-1,10-phenanthroline (5-Mephen), 4,7-dimethyl-1,10-phenanthroline (47-Me_2phen), 5,6-dimethyl-1,10-phenanthroline, 3,4,7,8-tetramethyl-1,10-phenanthroline (3,4,7,8-Me_4phen), Dowex 1X8-200, Amberlite IRA-400(Cl), DEAE-Sephadex A-25(Cl^-) anion exchange resin, and all cell culture reagents were purchased from Sigma Aldrich. Potassium tetrachloroplatinate(II) was purchased from Precious Metals Online. Dimethyl sulfoxide (DMSO-d_6, 99.9%) and deuterium oxide (D_2O, 99.9%) were purchased from Cambridge Isotope Laboratories. Cell culture vessels were purchased from Sarstedt. The caspase-3 substrate and inhibitor were purchased from Bachem. The ligand *rac*-bis(4-fluorophenyl)-1,2-ethylenediamine)platinum(II)] chloride (bfed) was synthesized by a previously published method.[16,30]

Calf thymus (ct-DNA, 42% G + C, mean molecular mass of $\sim 2 \times 10^7$) was prepared and characterized as described previously.[31] The polynucleotides were dissolved in 10 mM NaCl and kept frozen until the day of the experiment. HindIII and PvuII restriction endonucleases were purchased from New England Biolabs (Beverly, MA). Agarose was from FMC BioProducts (Rockland, ME). Wizard SV and PCR Clean-Up System used to extract and purify the DNA fragment was purchased from Promega (Madison, WI). Ethidium bromide (EtBr) was purchased from Merck KGaA, and deoxyribonuclease I (DNase I) was obtained from Roche (Mannheim, Germany). All other solvents were of analytical grade or higher and were used as received.

Nuclear Magnetic Resonance. ^1H and ^{19}F NMR spectra were obtained on a 300 MHz Varian Mercury, and ^{195}Pt spectra were obtained on a 400 MHz Bruker Avance spectrometer, either in DMSO-d_6 or D_2O, referenced internally to the solvent. ^{195}Pt spectra were externally referenced to K_2PtCl_4 at −1631 ppm. ^{19}F spectra were externally referenced to α,α,α-trifluorotoluene at 130 ppm. NMR experiments were run at 35 °C for DMSO and 25 °C for D_2O unless otherwise stated. For one-dimensional spectra, a spectral width of 5000 Hz was used with 50 000 data points and a relaxation delay of 3.7 s.

Elemental Analysis. Elemental analysis (C, H, and N) was used to determine the purity of the synthesized compounds, which in all cases was > 95%. Elemental analysis was conducted using a Carlo Erba 1106 automatic analyzer by the Microanalytical Unit, Research School of Chemistry, Australian National University.

Photodocumentation of HL-60 Cells. HL-60 cells were photographed with a Sony α100 digital camera mounted on a Carl Zeiss Axiovert25 inverse microscope with a 40 × 10 objective.

Synthesis of Platinum(II) Complexes. 1−**7** (Figure 1) were synthesized using a previously published method.[10] In brief, K_2PtCl_4 (∼0.2 g) was reacted with the ancillary ligand (A_L = *S*,*S*-dach or *R*,*R*-dach) (1 mol equiv) in water (∼ 30 mL), forming a yellow precipitate, which was filtered and washed with water, ethanol, and diethyl ether. The metal complex [Pt(A_L)Cl_2] was then reacted overnight with the intercalating ligand (I_L = phen, 5-Mephen, 5,6-Me_2phen, 4,7-Me_2phen, or 3,4,7,8-Me_4phen) (2 mol equiv) at reflux in H_2O (12−24 h, ∼200 mL). The volume was reduced (∼20 mL), and the excess intercalating ligand was removed using a Waters C18 reverse phase Sep-pak column (2 g), with the desired complex eluted with water and obtained by removal of the solvent under reduced pressure (yield ∼90%).

8−**12** were synthesized using an adaptation of published methods.[3,19,20] K_2PtCl_4 (∼0.2 g) and the intercalating ligand (I_L = phen, 5-Mephen, or 5,6-Me_2phen) (1 mol equiv) were stirred together in hot DMSO (30 mL), resulting in a clear yellow solution. When the mixture was cooled, a yellow precipitate formed, which was collected by vacuum filtration and washed with water, ethanol, and diethyl ether. The metal complex [Pt(I_L)Cl_2] was combined with the ancillary ligand (*S*,*S*-dped, *R*,*R*-dped, *rac*-bfed) (2 mol equiv) in H_2O (200−400 mL) and heated to reflux until the solution turned clear (24−48 h). The solution was filtered to remove any insoluble material. The filtrate was evaporated under reduced pressure to ∼50 mL. After the sample was removed from heat, saturated $NaClO_4$ solution (∼2 mL) was added and the resultant solution cooled, causing the precipitation of a white-yellow solid. The solvent was removed by vacuum filtration and the solid washed with water, ethanol, and diethyl ether (yield 80−90%). **8** and **9** were characterized and tested as the perchlorate salts, solubilized with DMSO.

10−**12** were converted to water-soluble salts by stirring, with gentle heating, in water (200 mL, 12 h) with DEAE Sephadex A-25 anion exchange resin (Cl^-). The Sephadex was removed by filtration, and yellow products were isolated by removal of the solvent under reduced pressure (yield ∼90%).

[(5,6-Dimethyl-1,10-phenanthroline)(1*S*,2*S*-diphenylethylenediamine)platinum(II)]$^{2+}$ Perchlorate (8). Yield 79%. Anal. Calcd for $C_{28}H_{28}Cl_2N_4O_8Pt$: C, 41.29; H, 3.46; N, 6.88%. Found: C, 41.06; H, 3.67; N, 6.80%. ^1H NMR (300 MHz, DMSO-d_6): δ

9.24 (d, 2H, J = 8.7 Hz), 9.18 (d, 2H, J = 4.8 Hz), 8.21 (dd, 2H, J = 5.4 Hz, J = 3.3 Hz), 7.75 (bs, 2H), 7.50 (d, 4H, 7.5 Hz), 7.32 (m, 6H), 6.99 (bs, 2H), 4.48 (s, 2H), 2.83 (s, 6H). ^{195}Pt NMR (85 MHz, DMSO-d_6): −2811 (bs).

[(5,6-Dimethyl-1,10-phenanthroline)(1*R*,2*R*-diphenylethylenediamine)platinum(II)]$^{2+}$ Perchlorate (9). Yield 83%. Anal. Calcd for $C_{28}H_{28}Cl_2N_4O_8Pt$: C, 41.29; H, 3.46; N, 6.88%. Found: C, 41.37; H, 3.60; N, 6.84%. ^{1}H NMR (300 MHz, DMSO-d_6): δ 9.24 (d, 2H, J = 8.7 Hz), 9.18 (d, 2H, J = 5.1 Hz), 8.21 (dd, 2H, J_1 = 5.4 Hz, J_2 = 3.3 Hz), 7.74 (bs, 2H), 7.50 (d, 4H, 6.9 Hz), 7.32 (m, 6H), 7.00 (bs, 2H), 4.48 (s, 2H), 2.83 (s, 6H). ^{195}Pt NMR (85 MHz, DMSO-d_6): −2811 (bs).

[(1,10-Phenanthroline)(1,2-bis(4-fluorophenyl)-1,2-ethylenediamine)platinum(II)]$^{2+}$ Chloride·[(1,10-phenanthroline)(1,2-bis-(4-fluorophenyl)-1,2-ethylenediamine)platinum(II)]$^{2+}$ Nickel(II) Tetrachloride, Tetrahydrate (10). {[Pt(phen)(*rac*-bfed)]Cl_2·[Pt-(phen)(*rac*-bfed)]$NiCl_4$}·4H_2O. Yield 85%. Anal. Calcd for $C_{55}H_{58}Cl_6F_4N_8NiO_5Pt_2$: C, 39.29; H, 3.30, N, 7.04%. Found: C, 38.99; H, 3.32, N, 7.27%. ^{1}H NMR (300 MHz, D_2O): 8.98 (d, 2H, J = 8.1 Hz), 8.97 (d, 2H, J = 4.5 Hz), 8.22 (s, 2H), 8.06 (dd, 2H, J_1 = 8.4 Hz, J_2 = 3.0 Hz), 7.52 (m, 4H), 7.15 (t, 4H, J = 9.0 Hz), 4.71 ppm (s, 2H). ^{19}F (282.1 MHz, D_2O): −133 ppm. ^{195}Pt (85 MHz, D_2O): −2820 (bs). Yellow crystals of **10** suitable for analysis by X-ray crystallography were obtained from water by slow diffusion by acetone over 3−4 days.

[(5-Methyl-1,10-phenanthroline)(1,2-bis(4-fluorophenyl)-1,2-ethylenediamine)platinum(II)]$^{2+}$ Chloride·[(5-methyl-1,10-phenanthroline)(1,2-*bis*(4-fluorophenyl)-1,2-ethylenediamine)platinum-(II)]$^{2+}$ Nickel(II) Tetrachloride, Hexahydrate (11). {[Pt(5-Mephen)(*rac*-bfed)]Cl_2·Pt(5-Mephen)(*rac*-bfed)]$NiCl_4$}·6H_2O. Yield 90%. Anal. Calcd for $C_{54}H_{60}Cl_6F_4N_8NiO_{14}Pt_2$: C, 36.38; H, 3.39; N, 6.29%. Found: C, 36.44; H, 3.22; N, 6.10%. ^{1}H NMR (300 MHz, D_2O): 9.09 (d, 1H, J = 8.4 Hz), 8.95 (d, 1H, J = 5.1 Hz), 8.87 (d, 1H, J = 8.1 Hz), 8.85 (d, 1H, J = 5.4 Hz), 8.08 (dd, 1H, J_1 = 8.4 Hz, J_2 = 3.3 Hz), 8.06 (s, 1H), 8.00 (dd, 1H, J_1 = 8.1 Hz, J_2 = 2.1 Hz), 7.52 (m, 4H), 7.14 (t, 4H, J = 8.7 Hz), 4.69 (s, 2H), 2.86 ppm (s, 3H). ^{19}F (282.1 MHz, D_2O): −133 ppm. ^{195}Pt (85 MHz, D_2O): −2820 (bs).

[(5,6-Dimethyl-1,10-phenanthroline)(*rac*-1,2-bis(4-fluorophenyl)-1,2-ethylenediamine)platinum(II)]$^{2+}$ Dichloride·3H_2O (12). Yield 90%. Anal. Calcd for $C_{28}H_{32}Cl_2F_2N_4O_3Pt$: C, 43.31; H, 4.15; N, 7.21%. Found: C, 43.22; H, 4.29; N, 6.99%. ^{1}H NMR (300 MHz, D_2O): 9.06 (d, 2H, J = 8.7 Hz), 8.87 (d, 2H, J = 4.8 Hz), 8.02 (dd, 2H, J_1 = 8.7 Hz, J_2 = 3.3 Hz), 7.52 (m, 4H), 7.14 (t, 4H, J = 8.7 Hz), 4.69 (s, 2H), 2.79 (s, 6H). ^{19}F (282.1 MHz, D_2O): −133 ppm. ^{195}Pt (85 MHz, D_2O): −2821 (bs).

Growth Inhibition Assays. All cancer cell lines were obtained from the German Collection of Microorganisms and Cell Culture (Braunschweig, FRG). Cell growth inhibition was measured as previously described.[22] Briefly, the antiproliferative effects of the complexes on the adherent cell lines (5637, RT-4, A427, LCLC-103H, DAN-G, and MCF-7) were measured by staining the cells with crystal violet after a 96 h exposure to the complexes. For the suspension cell line (HL-60), the MTT assay was used after exposing the cells to the complexes for 48 h. The MTT assay was also used for the A2780 cell line after exposing the cells to the complexes for 72 and 96 h. IC_{50} values were estimated by linear regression analysis of the log dose response curves with five serial dilutions of the complexes. IC_{50} values are averages of at least three independent experiments. The cisplatin resistant cell lines used in this work were created in vitro through repeated weekly exposures to cisplatin at increasing concentrations for 3 (SISO) to 5 (KYSE-70) months.

Caspase-3 Activation Assay. The activation of caspase-3-like activity in the HL-60 cell line was determined by the cleavage of a fluorogenic caspase-3 selective substrate as described in detail elsewhere.[32] Briefly, HL-60 cells were exposed to the compounds for 24 h, washed, lysed, and incubated (5 min, 30 °C) with the caspase-3 specific, irreversible inhibitor Z-DEVD-cmk (0 or 100 nM). Next, the cell lysate was incubated with the caspase-3 selective substrate Ac-DMQD-AMC (1 μM, 60 min, 30 °C). The amount of cleaved AMC after this time was quantified by an RP-HPLC assay. A small volume of sample (20 μL) was injected into a RP-HPLC system (Merck-Hitachi), and the AMC was separated on a C18 column (Macherey-Nagel CC250/4 Nucleosil 120-5 C18) with a mobile phase of 1:1 acetonitrile/water containing 0.1% trifluoroacetic acid and a flow rate of 0.7 mL/min. The column temperature was 30 °C. Retention time of AMC was 4.3 min. Quantification of AMC took place with a fluorescence detector (L-7485, Merck) that used an excitation wavelength of 355 or 400 nm and an emission wavelength of 435 nm. Calibration was performed with external standards of AMC. The difference between the amounts of AMC quantified in the cell lysates with and without and with inhibitor is equal to the specific activity of caspase-3 in HL-60 cells over 60 min. Untreated cells gave a background AMC release rate of 0.42 ± 0.08 (pmol/min)/mg protein. As a positive control, etoposide was incubated with HL-60 cells at 2 μM for 24 h, giving an AMC release rate of 3.37 ± 0.78 (pmol/min)/mg protein.

Cellular Platinum Uptake. The cellular platinum uptake rates were determined by using a method based on the AAS quantification of platinum in cell extracts as described in detail previously.[33] Briefly, 5637 cells (about 400 000) grown as a monolayer in 25 cm^2 flasks were treated with cisplatin or complexes **5** and **6** (25 μM) for 0, 2, 4, 6, or 8 h. After treatment, the monolayer was washed with PBS and a cell suspension was made by trypsinization. The cells were counted with a Z2 Coulter counter (Beckman-Coulter, Fullerton, CA) and then pelleted by centrifugation (5000g, 0 °C). The cell pellet was resuspended in PBS and pelleted again for storage (−20 °C). On the day of analysis, the pellets were thawed and resuspended in a solution of pancreatin (12 mg/mL) in phosphate buffer (63 mM, pH 6.8) and sonicated (15 min, 37 °C) to digest cell proteins. External standards of platinum were created in the same pancreatin solution. Cell samples (15 μL) were mixed with HNO_3 solution (5 μL, 0.5%) prior to analysis. Results are the average of three independent experiments. For flameless AAS analysis, a Unicam 989QZ AA spectrometer (Cambridge, U.K.) was used with deuterium compensation. The calibration and temperature program for the graphite oven were as previously described.[33]

Unwinding of Negatively Supercoiled DNA. Unwinding of closed circular supercoiled pSP73KB plasmid DNA was assayed by an agarose gel mobility shift assay.[24] The unwinding angle Φ, induced per platinum complex bound to DNA, was calculated upon the determination of the platinum/base ratio at which the complete transformation of the supercoiled to relaxed form of the plasmid was attained. The plasmid (79 μM; this concentration is related to the monomeric nucleotide content) was incubated (30 min, 25 °C) with increasing concentrations of the platinum complex in Tris-HCl (10 mM, pH 7.4). Subsequently, the samples were subjected to electrophoresis on 1% native agarose gel running at 25 °C in the dark with TAE (Tris-acetate/EDTA) buffer and the voltage set at 25 V. The gels were then stained with EtBr, followed by photography with a transilluminator.

Thermal stability of DNA. ct-DNA (10 mM, related to the monomeric nucleotide content) was incubated (30 min, 25 °C) with various concentrations of **5** and **6** in Tris-HCl (10 mM, pH 7.4). The melting curves of ct-DNA were then recorded by measuring the absorbance at 260 nm. The value of T_m was determined as the temperature corresponding to a maximum on the first-derivative profile of the melting curves. The T_m values could be thus determined with an accuracy of ±0.3 °C.

DNase I Footprinting. The 161 bp DNA fragment was prepared by digesting supercoiled pBluescript SK(−) phagemid (Stratagene, La Jolla, CA) with *Pvu*II and *Hind*III restriction endonucleases in the NEB buffer 2 supplied by the manufacturer and separated by electrophoresis in a 1% agarose gel made in

1× TBE buffer. The 161 bp fragment was isolated from the gel by Promega Wizard SV Gel Clean-Up System and 3′-end-labeled at the *Hind* III site by treatment with Klenow fragment (3′-5′ exo$^-$) of DNA polymerase I and [α-^{32}P]dATP. A 9 μL solution containing 1.11× TKMC buffer (10 mM Tris, pH 7.9, 10 mM KCl, 10 mM $MgCl_2$, and 5 mM $CaCl_2$), DNA (45 mM), and the studied compound was incubated (15 min at 25 °C). Cleavage was initiated by the addition of DNase I (1 μL of 50 μg/mL) and allowed to react for 30 s at room temperature before quenching with DNase stop solution (2.5 μL, 3 M NH_4OAc, 0.25 M EDTA). Optimal enzyme dilutions were established in preliminary calibration experiments. The sample was then precipitated with ethanol, lyophilized, and resuspended in a formamide loading buffer. DNA cleavage products were resolved by polyacrylamide (PAA) gel electrophoresis under denaturing conditions (8%/8 M urea PAA gel). The autoradiograms were visualized by using the BAS 2500 FUJIFILM bioimaging analyzer, and the radioactivities associated with bands were quantitated with the AIDA image analyzer software (Raytest, Germany). Assignment of the cleavage to a particular base has been made so that it corresponds to the cleavage of the phosphodiesteric bond on the 5′ side of that base.

Acknowledgment. The authors thank the University of Western Sydney for its financial support through internal research grants. A.M.K.-H. was supported by an Australian Postgraduate Award and a University of Western Sydney, College of Health and Science Publication Fellowship. The research of J.M., J.K., and V.B. was supported by the Ministry of Education of the CR (Grants MSMT LC06030, 6198959216, ME08017, OC08003, OC09018), the Academy of Sciences of the CR (Grants 1QS500040581, KAN-200200651, AV0Z50040507, and AV0Z50040702), and the Grant Agency of the Academy of Sciences of the CR (Grant IAA400040803). J.K. is International Research Scholar of the Howard Hughes Medical Institute.

Supporting Information Available: Figures showing crystal packing and structure; circular dichroism spectra. This material is available free of charge via the Internet at http://pubs.acs.org.

References

(1) Hollis, L. S.; Amundsen, A. R.; Stern, E. W. Chemical and biological properties of a new series of cis-diammineplatinum(II) antitumor agents containing three nitrogen donors: cis-[Pt(NH_3)$_2$-(N-donor)Cl]$^+$. *J. Med. Chem.* **1989**, *32*, 128–136.
(2) Farrell, N. Polynuclear platinum drugs. *Met. Ions Biol. Syst.* **2004**, *42*, 251–296.
(3) Brodie, C. R.; Collins, J. G.; Aldrich-Wright, J. R. DNA binding and biological activity of some platinum(II) intercalating compounds containing methyl-substituted 1,10-phenanthrolines. *Dalton Trans.* **2004**, 1145–1152.
(4) Jaramillo, D.; Buck, D. P.; Collins, J. G.; Fenton, R. R.; Stootman, F. H.; Wheate, N. J.; Aldrich-Wright, J. R. Synthesis, characterisation and biological activity of chiral platinum(II) complexes. *Eur. J. Inorg. Chem.* **2006**, *4*, 839–849.
(5) Wheate, N. J.; Brodie, C. R.; Collins, J. G.; Kemp, S.; Aldrich-Wright, J. R. DNA intercalators in cancer therapy: inorganic and organic drugs and their spectroscopic tools of analysis. *Mini-Rev. Med. Chem.* **2007**, *7*, 627–648.
(6) Kemp, S.; Wheate, N. J.; Buck, D. P.; Nikac, M.; Collins, G. J.; Aldrich-Wright, J. R. The effect of ancillary ligand chirality and phenanthroline functional group substitution on the cytotoxicity of platinum-based metallointercalators. *J. Inorg. Biochem.* **2007**, *101*, 1049–1058.
(7) Fisher, D. M.; Bednarski, P. J.; Grunert, R.; Turner, P.; Fenton, R. R.; Aldrich-Wright, J. R. Chiral platinum(II) metallointercalators with potent in vitro cytotoxic activity. *ChemMedChem* **2007**, *2*, 488–495.
(8) Fisher, D. M.; Fenton, R. R.; Aldrich-Wright, J. R. In vivo studies of a platinum(II) metallointercalator. *Chem. Commun.* **2008**, 5613–5615.
(9) Kemp, S.; Wheate, N. J.; Pisani, M. J.; Aldrich-Wright, J. R. Degradation of bidentate-coordinated platinum(II)-based DNA intercalators by reduced L-glutathione. *J. Med. Chem.* **2008**, *51*, 2787–2794.
(10) Wheate, N. J.; Taleb, R. I.; Krause-Heuer, A. M.; Cook, R. L.; Wang, S.; Higgins, V. J.; Aldrich-Wright, J. R. Novel platinum(II)-based anticancer complexes and molecular hosts as their drug delivery vehicles. *Dalton Trans.* **2007**, 5055–5064.
(11) Bednarski, P. J.; Gust, R.; Spruss, T.; Knebel, N.; Otto, A.; Farbel, M.; Koop, R.; Holler, E.; von Angerer, E.; Schonenberger, H. Platinum compounds with estrogen receptor affinity. *Cancer Treat. Rev.* **1990**, *17*, 221–231.
(12) Bednarski, P. J. Reactions of a cisplatin analog bearing an estrogenic 1,2-diarylethylenediamine ligand with sulfur-containing amino acids and glutathione. *Biochemistry* **1995**, *60*, 1–19.
(13) Schertl, S.; Hartmann, R. W.; Batzl-Hartmann, C.; Bernhardt, G.; Spruss, T.; Beckenlehner, K.; Koch, M.; Krauser, R.; Schlemmer, R.; Gust, R.; Schonenberger, H. [1,2-Bis(2,6-difluoro-3-hydroxyphenyl)ethylene-diamine]platinum(II) complexes, compounds for the endocrine therapy of breast cancer. Mode of action II: contribution of drug inactivation, cellular drug uptake and sterical factors in the drug−target interaction to the antitumor activity. *Arch. Pharm.* **2004**, *337*, 349–359.
(14) Reile, H.; Spruss, T.; Mueller, R.; Gust, R.; Bernhardt, G.; Schoenenberger, H.; Engel, J. Tumor-inhibiting [1,2-bis-(fluorophenyl)ethylenediamine]platinum(II) complexes. III. Evaluation of the mammary tumor-inhibiting properties. *Arch. Pharm.* **1990**, *323*, 301–306.
(15) Ott, I.; Gust, R. Preclinical and clinical studies on the use of platinum complexes for breast cancer treatment. *Anti-Cancer Agents Med. Chem.* **2007**, *7*, 95–110.
(16) Jennerwein, M.; Wappes, B.; Gust, R.; Schonenberger, H.; Engel, J.; Seeber, S.; Osieka, R. Influence of ring substituents on the antitumor effect of dichloro(1,2-diphenylethylenediamine)-platinum(II) complexes. *J. Cancer Res. Clin. Oncol.* **1988**, *114*, 347–358.
(17) Wappes, B.; Jennerwein, M.; Von Angerer, E.; Schoenenberger, H.; Engel, J.; Berger, M.; Wrobel, K. H. Dichloro[1,2-bis(4-hydroxyphenyl)ethylenediamine]platinum(II) complexes: an approach to develop compounds with a specific effect on the hormone-dependent mammary carcinoma. *J. Med. Chem.* **1984**, *27*, 1280–1286.
(18) Schertl, S.; Hartmann, R. W.; Batzl-Hartmann, C.; Bernhardt, G.; Spruss, T.; Beckenlehner, K.; Koch, M.; Krauser, R.; Schlemmer, R.; Gust, R.; Schonenberger, H. [1,2-Bis(2,6-difluoro-3-hydroxyphenyl)ethylenediamine]platinum(II) complexes, compounds for the endocrine therapy of breast cancer mode of action I: antitumor activity due to the reduction of the endogenous estrogen level. *Arch. Pharm.* **2004**, *337*, 335–348.
(19) Brodie, C. R.; Turner, P.; Wheate, N. J.; Aldrich-Wright, J. R. (4,7-Dimethyl-1,10-phenanthroline)(ethylenediamine)platinum(II) dichloride tris(deuterium oxide) solvate. *Acta Crystallogr., Sect. E* **2006**, *E62*, m3137–m3139.
(20) McFadyen, W. D.; Wakelin, L. P. G.; Roos, I. A. G.; Leopold, V. A. Activity of platinum(II) intercalating agents against murine leukemia L1210. *J. Med. Chem.* **1985**, *28*, 1113–1116.
(21) Kato, M.; Takahashi, J. Anion-controlled -stacks of (ethylenediamine-*N*,*N*′)(1,10-phenanthroline-*N*,*N*′)platinum(II). *Acta Crystallogr.* **1999**, *C55*, 1809–1812.
(22) Bracht, K.; Boubakari; Grünert, R.; Bednarski, P. J. Correlations between the activities of 19 anti-tumor agents and the intracellular glutathione concentrations in a panel of 14 human cancer cell lines: comparisons with the National Cancer Institute data. *Anti-Cancer Drugs* **2006**, *17*, 41–51.
(23) Schertl, S.; Hartmann, R. W.; Batzl-Hartmann, C.; Bernhardt, G.; Spruss, T.; Beckenlehner, K.; Koch, M.; Krauser, R.; Schlemmer, R.; Gust, R.; Schonenberger, H. [1,2-Bis(2,6-difluoro-3-hydroxyphenyl)ethylenediamine]platinum(II) complexes, compounds for the endocrine therapy of breast cancer. Mode of action I: antitumor activity due to the reduction of the endogenous estrogen level. *Arch. Pharm.* **2004**, *337*, 335–348.
(24) Keck, M. V.; Lippard, S. J. Unwinding of supercoiled DNA by platinum−ethidium and related complexes. *J. Am. Chem. Soc.* **1992**, *114*, 3386–3390.
(25) Jennette, K. W.; Lippard, S. J.; Vassiliades, G. A.; Bauer, W. R. Metallointercalation reagents. 2-Hydroxyethanethiolato(2,2′,2″-terpyridine)platinum(II) monocation binds strongly to DNA by intercalation. *Proc. Natl. Acad. Sci. U.S.A.* **1974**, *71*, 3839–3843.
(26) Novakova, O.; Chen, H.; Vrana, O.; Rodger, A.; Sadler, P. J.; Brabec, V. DNA interactions of monofunctional organometallic ruthenium(II) antitumor complexes in cell-free media. *Biochemistry* **2003**, *42*, 11544–11554.
(27) Maeda, Y.; Nunomura, K.; Ohtsubo, E. Differential scanning calorimetric study of the effect of intercalators and other kinds of

DNA-binding drugs on the stepwise melting of plasmid DNA. *J. Mol. Biol*. **1990**, *215*, 321–329.
(28) Bjorndal, M. T.; Fygenson, D. K. DNA melting in the presence of fluorescent intercalating oxazole yellow dyes measured with a gel-based assay. *Biopolymers* **2002**, *65*, 40–44.
(29) Fairall, L.; Rhodes, D. A new approach to the analysis of DNase I footprinting data and its application to the TFIIIA/5S DNA complex. *Nucleic Acids Res*. **1992**, 20.
(30) Vogtle, F.; Goldschmitt, E. Die diaza-cope-umlagerung. *Chem. Ber*. **1976**, *109*, 1–40.
(31) Brabec, V.; Palecek, E. Interaction of nucleic acids with electrically charged surfaces. II. Conformational chances in double-helical polynucleotides. *Biophys. Chem*. **1976**, *4*, 76–92.
(32) Vogel, S.; Kaufmann, D.; Pojarová, M.; Müller, C.; Pfaller, T.; Kühne, S.; Bednarski, P. J.; Angerer, E. v. Aroyl hydrazones of 2-phenylindole-3-carbaldehydes as novel antimitotic agents. *Bioorg. Med. Chem*. **2008**, *16*, 6436–6447.
(33) Bednarski, P. J.; Grünert, R.; Zielzki, M.; Wellner, A.; Mackay, F. S.; Sadler, P. J. Light-activated destruction of cancer cell nuclei by platinum diazide complexes. *Chem. Biol*. **2006**, *13*, 61–67.